Drug Design, Development and Therapy

Dovepress

open access to scientific and medical research

Open Access Full Text Article

ORIGINAL RESEARCH

Cerebral protection of epigallocatechin gallate (EGCG) via preservation of mitochondrial function and ERK inhibition in a rat resuscitation model

This article was published in the following Dove Press journal:
Drug Design, Development and Therapy

Sina Qin*
Meng-hua Chen*
Wei Fang
Xiao-feng Tan
Lu Xie
Ye-gui Yang
Tao Qin
Nuo Li

Intensive Care Unit, The Second Affiliated Hospital of Guangxi Medical University, Nanning, Guangxi, People's Republic of China

*These authors contributed equally to this work

Background: Various and opposite roles of epigallocatechin gallate (EGCG) have been reported in different studies. We aimed to investigate how EGCG affects the cerebral injury in a cardiac arrest/cardiopulmonary resuscitation (CA/CPR) model of rat.

Methods: The rats which were subjected to CA/CPR randomly received low dose of EGCG (3 mg/kg, Low-EGCG group, n=16), high dose of EGCG (9 mg/kg, High-EGCG group, n=16) and equal volume of 0.9% saline solution (NS group, n=16) at the first minute after return of spontaneous circulation (ROSC). The rats underwent anesthesia and intubation were defined as Sham group (n=16). Twenty-four hours after ROSC, neural defect score (NDS), ROS fluorescence intensity, degree of mitochondrial permeability transition pore (mPTP) opening, ATP contents and mitochondrial ATP synthase expression were evaluated in the four groups. The expression of extracellular signal-regulated kinase (ERK) activity and cleaved-caspase 3 were also detected by Western blot.

Results: CA/CPR induced severe ischemia-reperfusion injury (IRI), resulted in mitochondrial dysfunction and upregulated phosphorylation of ERK. EGCG dose-dependently alleviated the IRI after CA/CPR, inhibited ERK activity and restored mitochondrial function and, as indicated by improved NDS, reduced ROS level, decreased mPTP opening, elevated ATP content, increased ATPase expression and downregulated cleaved-caspase 3 level.

Conclusion: EGCG alleviated global cerebral IRI by restoring mitochondrial dysfunction and ERK modulation in a rat CA/CPR model, which might make it a potential candidate agent against IRI after CA/CPR in the future. Further study is needed to determine whether higher dosage of EGCG might aggravate cerebral IRI post-CA/CPR.

Keywords: EGCG, CA/CPR, ischemia-reperfusion injury, mitochondrial permeability transition pore, ATP, ERK

Introduction

As cerebral ischemia occurs, it is important to restore blood perfusion timely and efficiently because brain is vulnerable without perfusion within a few minutes. Prolonged ischemia and delayed reperfusion could result in more serious injury which is known as ischemia-reperfusion injury (IRI).[1,2] Cardiac arrest (CA) causes systemic ischemia. Despite the successful restoration of spontaneous circulation, there were still a subset of patients suffered from cerebral IRI.[3,4] This situation raised the worldwide concern.[5,6]

Correspondence: Nuo Li
Intensive Care Unit, The Second Affiliated Hospital of Guangxi Medical University, 166# Eastern University Road, Nanning, Guangxi, People's Republic of China
Tel +86 0 771 327 7186
Email 120159659@qq.com

submit your manuscript | www.dovepress.com
DovePress
http://doi.org/10.2147/DDDT.S215358

Cerebral protection by mild hypothermia after CA and cardiopulmonary resuscitation (CA/CPR) is generally accepted by clinicians.[7] Preservation of energy substances has been recognized as one of the mechanisms by which hypothermia treatment exerts its cerebral protective role.[8] ATPis a complex organic chemical that provides energy to drive many physiological processes in living cells. Excessive ATP depletion is associated with cell apoptosis.[9] Therefore, it is reasonable to propose that mitochondria, the major source of ATP, may be a potential therapy target for IRI.

Epigallocatechin gallate (EGCG) is the most effective bioactive component of tea polyphenols. It shows many benefit roles revealing as cardio protection, anticancer and diabetes.[10–12] EGCG can accumulate in mitochondria and have direct actions on it.[13] Zheng and Ramirez demonstrated that EGCG played a pro-apoptosis role, as described by inhibiting the activity of ATP synthase and inducing openness of mitochondrial permeability transition pore (mPTP).[14] By contrast, studies by Dragicevic and Krishnan showed that EGCG maintained mitochondrial function and restored Bcl-2 protein levels, contributing to an anti-apoptotic effect.[15,16] There are many reasons account for the opposing roles of EGCG, such as different dosages, cellular conditions and cell types. Hence, it is necessary to determine the effect of EGCG at certain dosage in each specific pathology conditions under the initiative of precision medicine.

CA/CPR model presents global cerebral injury and closely mimics the clinical condition. It is helpful for pharmacodynamics study. Our previous studies showed that animals with severe IRI after CA/CPR presented excessive phosphorylation of extracellular signal-regulated kinase (ERK). The downregulation of phosphorylated ERK (p-ERK) by PD98059, a specific ERK inhibitor, significantly improved the adverse outcome.[17,18] On the other hand, focal cerebral damage model established by middle cerebral artery occlusion (MCAO) could simulate the condition of stroke and it also can be used in cerebral IRI studies. However, the injury mechanism of MCAO model may be different from that involved in cerebral damage after CA/CPR. The depressed expression of p-ERK was observed in rats subjected to MCAO in multiple studies, while the experimental intervention which restored p-ERK level could alleviate the cerebral damage.[19–21]

By now few studies can answer the question that whether EGCG can exert a protective effect on mitochondria in brain tissue in a CA/CPR model. Therefore, we aimed to verify this hypothesis in this study.

Experimental procedures

Animal preparation and a rat cerebral ischemia-reperfusion model induced by CA/CPR

Healthy adult male Sprague-Dawley (SD) rats (body weight 230–260 g) were provided by the Experimental Animal Center of Guangxi Medical University. All rats were handled according to the Guidelines for the Care and Use of Laboratory Animals of the National Institute of Health and the experimental protocol was approved by the Animal Experiment Committee of Guangxi Medical University. The laboratory temperature was maintained at 26°C. Rats were fasted for 12 hrs with access to water ad libitum before surgery. And then the rats were anesthetized with intraperitoneal injection of 2% pentobarbital sodium (Serva, Germany) (30 mg/kg) before operation. The anesthetized SD rats were immobilized on a small surgical board. The skin of anterior portion of neck and left groin area were sterilized. The trachea was exposed by blunt separation. The left femoral artery and vein were separated and intubated with a PE-50 silica gel tube (Becton-Dickinson, Franklin Lakes, NJ, USA) filled with 5 IU/mL heparin sodium solution. A pressure transducer (Chengdu Taimeng Instrument Co. Ltd., People'sRepublic of China) was connected with the femoral artery lien tube for blood pressure monitoring and the vein intubation was for medicine administration. Three needle electrodes (Chengdu Taimeng Instrument Co. Ltd.) were placed subcutaneously on both upper limbs and the right lower limb respectively, and the standard II lead electrocardiogram was recorded with the record speed of 250 ms/div. All the data was obtained by BL-420F biological system (Chengdu Taimeng Instrument Co. Ltd.). The rectum temperature of rats was maintained at 37.0±0.5°C with a heating lamp. After the arterial pressure and electrocardiogram were stabilized for 10 mins, the CA was induced by transoesophageal electrical induction according to our previous report.[22] Seven minutes after CA induction, the CPR was initiated with a mechanical chest compressor (LUCAS Chest Compression System; Jolife AB, Mantzaris, Greece). The chest compression depth was one-third of the anterior and posterior diameter of the rat's chest with the frequency 180/min. Meanwhile, the mechanical ventilation (Shanghai Alcott Biotechnology Co., Ltd., People's Republic of China) was started with the tidal volume 6 mL/kg and the ventilation frequency 72/min. One minute after CPR initiation, epinephrine (Shanghai Wellhope Pharmaceutical Co., Ltd., People's Republic of

China) at a dosage of 0.02 mg/kg was delivered via vein tube followed by chest compression if return of spontaneous circulation (ROSC) was not obtained. The additional equal volume of epinephrine was administrated after 3 mins of compression if ROSC was not achieved. The ROSC was defined as supraventricular rhythm and the mean arterial pressure was >50 mmHg, which lasted for more than 5 mins. Rats failed to obtain ROSC after 10 mins of CPR were excluded.

Two different concentrations of EGCG solution, 1.25 mg/mL (EGCG-A solution) and 3.75 mg/mL (EGCG-B solution), were purchased from Shanghai Yuanye Bio-Technology Co., Ltd, People's Republic of China. The rats which obtained ROSC within 3 mins randomly received EGCG-A solution (Low-EGCG group, n=16), EGCG B solution (High-EGCG group, n=16) or 0.9% normal saline solution at a dose of 2.4 mL/Kg, respectively. Therefore, the total dosage of EGCG delivered to Low-EGCG group was 3 mg/kg while the High-EGCG group 9 mg/kg. Arterial blood pressure and electrocardiogram were continually monitored for 1 hr. The rats subjected to only anesthesia and intubation were defined as Sham group. After 1 hr of observation, the rats with stable hemodynamics were placed alone in a cage with dry bedding and housed in an air-conditioned and peaceful room (temperature 26°C). They had free access to water and food.

The time from CPR to ROSC and neurological deficit score after ROSC 24 hrs

The time from CPR initiation to ROSC was recorded. At 24 hrs after ROSC, neurologic function scores evaluation was conducted. The neurological deficit scores (NDS) measure the level of arousal, cranial nerve reflexes, motor function and simple behavioral responses. The neurologic deficits were scored from 0 (death or brain death) to 80 (no observed neurologic deficit).[23] Two independent investigators measured the NDS in this evaluation and reached an agreement.

ROS measurement

Dihydroethidium (DHE; Sigma-Aldrich, USA) was used as an ROS-specific fluorescent probe; DHE and intracellular ROS form ethyl oxide species that can mix with chromosomal DNA to produce red fluorescence, the measurement of which provides an estimate of cellular ROS content. At 24 hrs after reperfusion, the rats (n=8 for each group) were anesthetized with an intraperitoneal injection of 2% pentobarbital sodium (30 mg/kg). Then, the brains were removed quickly, frozen and cut into 5-μm-thick sections using a CM1950 Cryostat Microtome (Leica, Nussloch, Germany), fixed by acetone, and then incubated with 1 μmol/L DHE for 30 mins at 37°C. After incubation, fluorescence was observed using a confocal laser microscope (A1; Nikon, Tokyo, Japan) at an excitation wavelength of 488 nm, and emission was recorded at 543 nm. Images were captured by the confocal laser microscope and were set at 1024×1024 pixels using a ×20 objective lens. The fluorescence intensity of ethidium-positive cells was quantified by NIS-Elements AR3.2 64-bit image software.

Measurement of mitochondrial permeability

At 24 hrs after ROSC, the rats (n=8 for each group) were anesthetized with intraperitoneal injection of 2% pentobarbital sodium. Then, the brains were quickly removed for mitochondria isolation. Determination of mPTP opening was performed with an MPTP Fluorescence Detection Kit (GENMED Scientifics, Inc. People'sRepublic of China). Calcein-AM is a dye that selectively aggregates inside mitochondria and produces green fluorescence. The dye is released from the mitochondria when the mPTP opens, and changes in mitochondrial fluorescence reflect the degree of mPTP opening. The fluorescence intensity of mitochondria was determined using a microplate reader (Synergy H1; BioTek, Winooski, VT, USA) at an excitation wavelength of 488 nm and emission wavelength of 505 nm. Mitochondrial protein was quantified using a commercial kit (GENMED Scientifics, Inc.); mitochondrial fluorescence was calculated relative to protein concentration (n=8/group). The lower the mitochondrial calcein fluorescence, the greater the opening of the mitochondrial membrane channel hole (mPTP).

Determination of brain ATP contents

At 24 hrs after ROSC, the rats (n=8/group) were anesthetized with intraperitoneal injection of 2% pentobarbital sodium. Then, the brains were quickly removed. About 60 mg cerebral cortex tissues were collected and homogenized with 600 μL ATP detection cracking solution according to ATP detection kit (S0026, Beyotime Biotechnology Co. Ltd., Shanghai, People's Republic of China). The brain tissue homogenate was centrifuged at

12,000 g at 4°C for 5 mins. The supernatant was then used for the measurement of brain ATP contents according to ATP detection kit. Fluorescein in the ATP detection reagent uses the energy provided by ATP to produce fluorescein, which is directly proportional to the concentration of ATP, and uses a chemiluminescence detector (Luminometer) to detect fluorescence. Tissue protein was quantified using the Coomassie brilliant blue reagent (Nanjing Jian Cheng Technology, People's Republic of China), and contents of ATP were calculated relative to the mass of protein (n=8 for each group).

Assessment of ATP synthase

At 24 hrs after ROSC, the rats (n=8/group) were anesthetized with intraperitoneal injection of 2% pentobarbital sodium. Then, the brains were quickly removed. A quantity of 60 mg cerebral cortex tissue was taken, blood was washed with 1×PBS solution, and 600 μL1×PBS was added to make homogenate. The brain tissue homogenate was placed at −20°C refrigerator overnight. After repeated freezing and thawing for two times, the brain tissue homogenate was centrifuged at 5000 g at 4°C for 5 mins. The supernatant was then used for the measurement of brain ATP synthase (ATP5C1) according to Rat ATP synthase subunit ELISA kit (Wuhan Huamei Biological Engineering Co. Ltd., People's Republic of China). The absorbance (OD) value was determined by 450 nm wavelength multifunctional enzyme spectrometer (BIOTEK Synergy H1, USA), and the concentration of the sample ATP synthase (ATP5C1) was calculated. Tissue protein was quantified using the Coomassie brilliant blue reagent (Nanjing Jian Cheng Technology), and ATP synthase (ATP5C1) contents were calculated relative to the mass of protein (n=8 for each group).

Western blot detection

The expression of cleaved-caspase 3, total ERK (t-ERK) and (p-ERK were assessed by Western blotting. Cerebral tissues were collected, weighed and homogenized in a 1:10 (w/v) radio immunoprecipitation assay lysis buffer (P0013B; Beyotime Biotechnology) including a 1 mmol/L phenylmethanesulfonyl fluoride (P0100; Solarbio, Beijing, People's Republic of China) solution using a gslass homogenizer. After 30 min, the soluble proteins were collected and centrifuged at 14,000× g for 15 mins at 4°C and then denatured at 100°C for 15 mins in 4× SDS-PAGE loading buffer (P1015; Solarbio). Equal amounts of the proteins (20 μg) from each sample were separated by 15% SDS-PAGE and transferred onto Immobilon-P membranes (0.22 μm bore diameter; Millipore, Bedford, MA, USA), which was then blocked by 5% nonfat milk. Immunoblotting analysis was performed using an anti-ERK/p-ERK monoclonal antibody (#9662, 1:800; Cell Signaling Technology, Danvers, MA, USA) and cleaved-caspase-3 monoclonal antibody (#9662, 1:800; Cell Signaling Technology). β-Actin was used to control for equal sample loading in each subcellular fraction (#8457, 1:1000; Cell Signaling Technology). Then, the membranes were washed with Tris-buffered saline containing 0.1% Tween 20 (TBST) and incubated for 2 hrs with a secondary antibody (#5151, 1:15,000; Cell Signaling Technology) at room temperature. Finally, the membranes were washed in TBST and the optical densities of the protein bands were analyzed by Odyssey (LI-COR Biosciences, Lincoln, NE, USA). Blot bands were quantified with Image J software (v1.33; NIH, USA). All data were obtained from three independent experiments.

The expression of cleaved-caspase 3, t-ERK and p-ERK were assessed by Western blotting. Cerebral tissues were collected, weighed and homogenized in a 1:10 (w/v) radio immunoprecipitation assay lysis buffer (P0013B; Beyotime Biotechnology) including a 1 mmol/L phenylmethanesulfonyl fluoride (P0100; Solarbio) solution using a glass homogenizer. After 30 mins, the soluble proteins were collected and centrifuged at 14,000× g for 15 mins at 4°C. After centrifugation, total protein concentration was determined using a BCA Protein Assay Reagent Kit (P0010; Beyotime Biotechnology, USA) with the proteins extracted from the supernatant, which were then denatured at 100°C for 15 mins in 4× SDS-PAGE loading buffer (P1015; Solarbio). Samples containing 20 μg total protein were separated by 15% SDS-PAGE and transferred to an Immobilon-P membrane (0.22 μm bore diameter; Millipore), which was then blocked by 5% nonfat milk. Immunoblotting analysis was performed using anti-ERK monoclonal antibody (#4695, 1:1000, Cell Signaling Technology), p-ERK monoclonal antibody (#9101, 1: 1000; Cell Signaling Technology) and cleaved-caspase-3 monoclonal antibody (#9662, 1:800; Cell Signaling Technology). β-Actin was used to control for equal sample loading in each subcellular fraction (#8457, 1:1000; Cell Signaling Technology). After three washes for 5 mins with Tris-buffered saline containing 0.1% Tween 20 (TBST), the membranes were further incubated with a secondary antibody (#5151, 1:15,000; Cell Signaling Technology) for 2 hrs followed by three washes with TBST. The optical densities of the protein bands were analyzed by Odyssey (LI-COR Biosciences). Blot bands

were quantified with Image J software (v1.33; NIH). All data were obtained from three independent experiments.

Statistical analysis

Analysis of data was performed using SPSS 22.0 statistical software. Groups were compared using one-way ANOVA followed by the Student–Newman–Keul test or Dunn–Bonferroni approach for post hoc comparisons. All data were expressed as the mean±SD, and the value of $p<0.05$ was considered to indicate a statistically significant difference.

Results

The time to ROSC and neurological deficit score (NDS) after ROSC 24 hrs

We record the duration from the initiation of CPR to ROSC. There was no statistically significant difference among the NS group, the Low-EGCG group and High-EGCG group ($P>0.05$) (Table 1). This result indicated that the ischemic duration of the three groups is consistent. At 24 hrs after ROSC, the NDS evaluation was conducted in all groups. EGCG dose-dependently improved the neural function; however, the difference among the three groups was not significant ($p>0.05$) (Table 1).

EGCG reduced the content of ROS

As an ROS-specific fluorescent probe, DHE can be used to indicate the oxidative stress level. The ROS level assessment was performed at 24 hrs after ROSC. The ROS fluorescence staining pictures in the four groups are shown in Figure 1A, and the fluorescence density of ROS in the four groups is compared in Figure 1B. Compared with the Sham group, the ROS fluorescence density of the NS group was significantly increased ($P<0.01$). By contrast, EGCG reduced the ROS content in a dose-dependent manner, as indicated by decreased ROS fluorescence density in the Low-EGCG group ($p<0.05$) and High-EGCG group ($p<0.01$), respectively. In addition, the High-EGCG group showed enhanced anti-oxidative role compared with the Low-EGCG group ($p<0.05$).

Table 1 Time to ROSC and NDS after ROSC 24 hrs

Group	n	Time to ROSC (s)	NDS
Sham	16	-	80
NS	16	105.8±40.8	75.4±1.6
Low-EGCG	16	109.7±31.4	76.0±1.5
High-EGCG	16	105.8±32.8	76.7±1.4

Abbreviations: NDS, neurological deficit score; ROSC, return of spontaneous circulation.

EGCG attenuated MPTP opening

Mitochondrial fluorescence intensity reflects the degrees of mPTP opening. Lower intensity indicates increased opening of mPTP, which could allow more cytochrome c release thereby initiating cellular apoptosis process.

Figure 2 presents the comparison of the degree of mPTP in all groups. The fluorescence intensity of NS group was significantly decreased compared with the Sham group ($p<0.01$). Low dose of EGCG improved the opening of mPTP, although there was no statistical difference ($p>0.05$). Treatment with high dose of EGCG attenuated mPTP opening ($p<0.05$), and its positive effect was better than that contributed from low dose of EGCG ($p<0.05$) (Figure 2).

EGCG restored brain ATP level

ATP is generated in mitochondria. Partial ATP depletion may induce apoptosis. Therefore, ATP level could be an indicator for mitochondrial function and cerebral injury. At 24 hrs after ROSC, the ATP level was obviously decreased in NS group ($p<0.01$). EGCG dose-dependently restored the mitochondrial function and decreased cerebral injury, as indicated by increased ATP content in the Low-EGCG group ($p<0.05$) and High-EGCG group ($p<0.01$), respectively (Figure 3).

EGCG increased brain ATP synthase (ATP5C1) expression

The level ATP synthase (ATP5C1) expression links to ATP generation and reflects the mitochondrial function. Rats subjected to CA/CPR significantly hampered the expression of ATPase ($p<0.01$). In the High-EGCG group, obvious upregulation of ATPase was observed ($p<0.01$), while low dose of EGCG increased ATPase expression without statistical difference. As shown in Figure 4, the positive effect of high dose of EGCG was better than that derived from the lower (Figure 4).

Western blot detection

ERK pathway and cleaved-caspase 3 play important roles in the regulation of cell apoptosis. We detected ERK activation and cleaved caspase 3 expression to explore the effect and its mechanism of EGCG in IRI at 24 hrs after ROSC. Figures 5 (A and B) present the

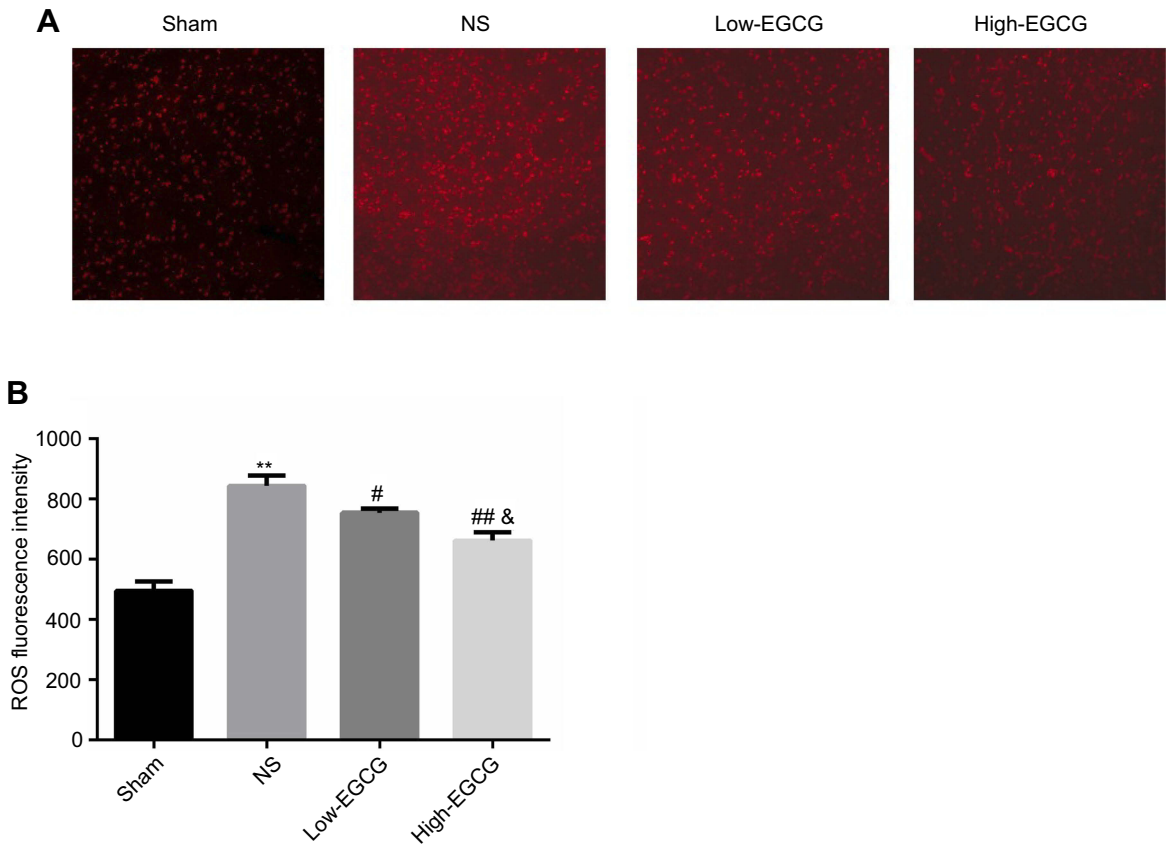

Figure 1 (**A**). The brain ROS fluorescence staining images of the rats in the four groups. (**B**). Comparison of the brain ROS fluorescence intensity in the four groups. Data are expressed as mean±SD. $p^{**}<0.01$ compared with the Sham group; $p^{\#\#}<0.01$ compared with the NS group; $p^{\#}<0.05$ compared with the NS group; $p^{\&}<0.05$ compared with the Low-EGCG group (n=8 for each group).
Abbreviations: EGCG, epigallocatechin gallate; ROS, reactive oxygen species.

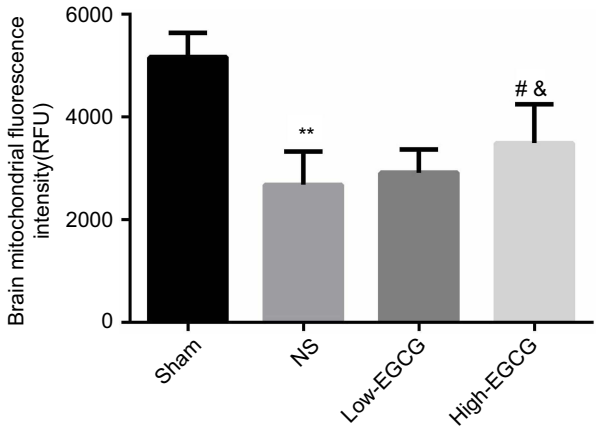

Figure 2 Comparison of the cerebral mitochondrial fluorescence intensity in the four groups. Data are expressed as mean±SD. $p^{**}<0.01$ compared with the Sham group; $p^{\#}<0.05$ compared with the NS group; $p^{\&}<0.05$ (n=8 for each group).
Abbreviations: EGCG, epigallocatechin gallate; mPTP, mitochondrial permeability transition pore.

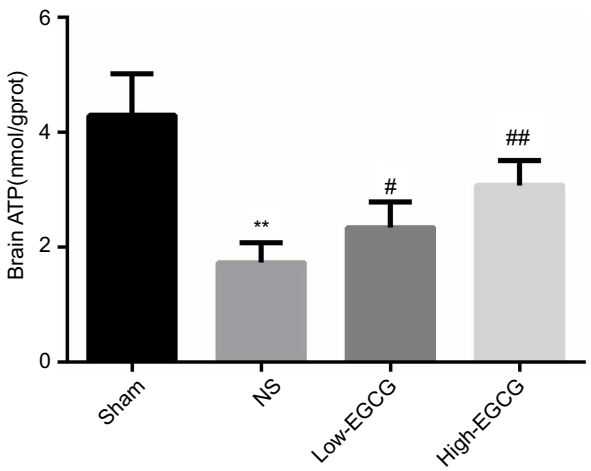

Figure 3 The ATP content in the four groups. Data are expressed as mean±SD. $p^{**}<0.01$ compared with the Sham group; $p^{\#}<0.05$ compared with the NS group; $p^{\#\#}<0.01$ compared with the NS group (n=8 for each group).
Abbreviations: EGCG, epigallocatechin gallate; ATP, adenosine triphosphate.

Western blot of p-ERK, t-ERK and cleaved-caspase 3, respectively. The results showed that the elevated expression of p-ERK and cleaved-caspase 3 were detected in the rats subjected to CA/CPR. EGCG significantly inhibited ERK activity ($p<0.01$) and down-regulated cleaved-caspase 3 expression ($p<0.05$) in a dose-dependent manner Figure 5 (C and D).

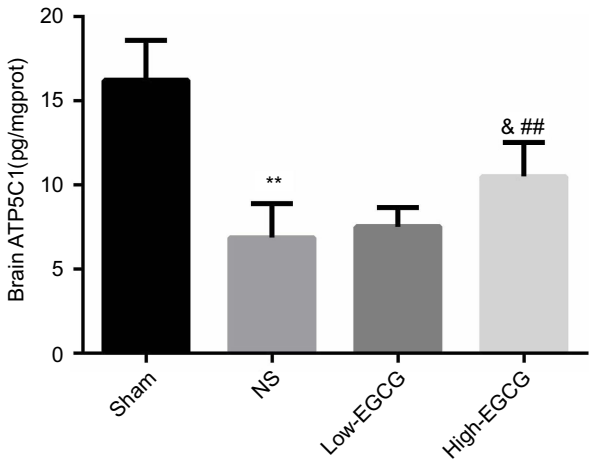

Figure 4 Comparison of the brain ATPase content in the four groups. Data are expressed as mean±SD. p^{**}<0.01 compared with the Sham group; $p^{\#\#}$<0.01 compared with the NS group; $p^{\&}$<0.05 compared with Low-EGCG group. (n=8 for each group).
Abbreviations: EGCG, epigallocatechin gallate; ATPase, adenosine triphosphate synthase.

Discussion

Cerebral injury post-CA/CPR raises a worldwide concern. Multiple therapies have been suggested, yet the situation is still challenging.[3,5,6] Novel and effective approach dealing with cerebral injury post-CA/CPR is imperative. In our current study, rats subjected to CA/CPR present severe IRI, as indicated by worse neural defect scores, elevated reactive oxygen species level, compromise mitochondrial structure and bioenergetics as well as increased apoptosis compared with the Sham group. Treatment with EGCG dose-dependently improves these adverse outcomes. As far as we know, this is the first study in vivo focusing on the effect of EGCG on cerebral protection in rat post-CA/CPR.

In mitochondria, electron transport chain (ETC) consists with a series of enzyme and is responsible for most mitochondrial functions via redox reactions.[24] On one hand, adenosine triphosphate synthase (ATPase) is known as respiratory chain complex V which is a key enzyme in ETC. It is the only diffusion channel of proton in mitochondria. Coupled with the redox reaction, ETC pumps protons from the mitochondrial matrix to the intermembrane space to form an electrochemical gradient. Subsequently, the electrical potential energy produced by proton concentration gradient promotes the ATP synthase with assistance of the ATPase. On the other hand, a small quantity of electrons leak from the ETC and then combine with oxygen molecules to generate a low level of ROS.[25] In case of ischemia, electrons accumulate in ETC due to its transfer function failure. In reperfusion phase, blood brings a large amount of oxygen molecules, which combine with the electrons stay in ETC previously to form

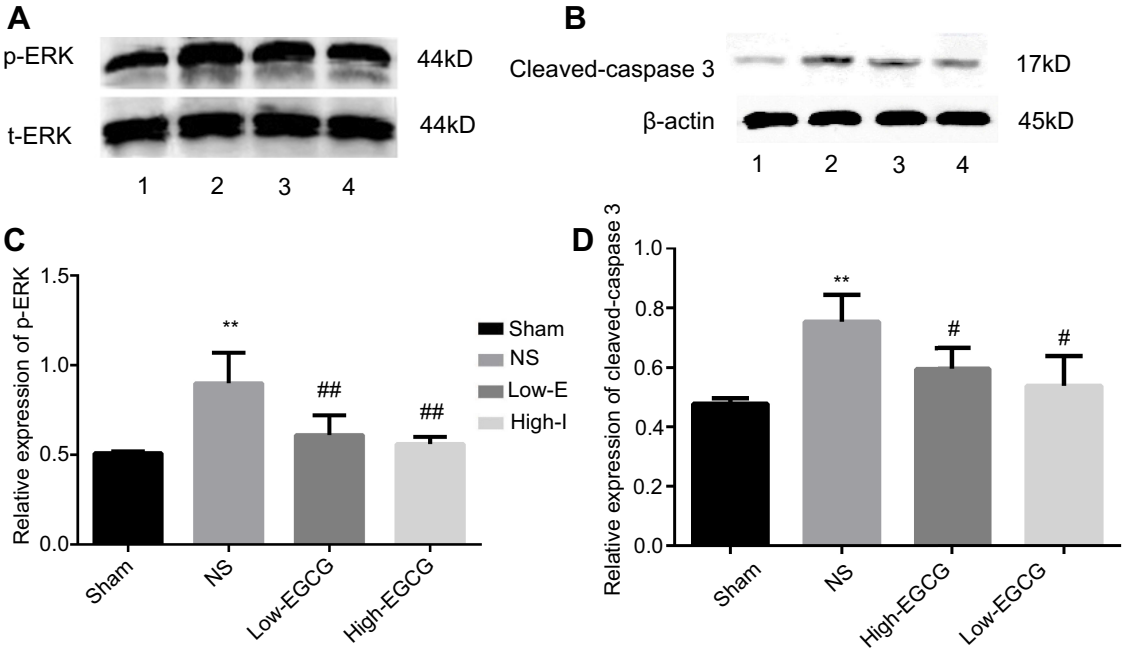

Figure 5 (A) The Western blot of p-ERK and ERK in the four groups: 1) Sham group; 2) NS group; 3) Low-EGCG group; 4) High-EGCG group. **(C)** The comparison of p-ERK in the four groups. Data are expressed as mean±SD. p^{**}<0.01 compared with the Sham group; $p^{\#\#}$<0.01 compared with the NS group (n=8 for each group). **(B)** The Western blot of cleaved-caspase 3 in the four groups: 1) Sham group; 2) NS group; 3) Low-EGCG group; 4) High-EGCG group. **(D)** The comparison of cleaved-caspase 3 in the four groups. Data are expressed as mean±SD. p^{**}<0.01 compared with the Sham group; $p^{\#}$<0.05 compared with the NS group (n=8 for each group).
Abbreviations: EGCG, epigallocatechin gallate; ERK, extracellular signal regulated kinase.

excessive ROS. ROS burst will trigger the opening of mPTP which will in turn impair mitochondrial bioenergetics causing mitochondria swelling and ATP depletion and promote cytochrome c release thereby initiating cellular apoptosis process. In the present study, we chose 24 hrs after ROSC as the evaluation time point since our previous study results showed that among all the observation point, animals which underwent CA/CPR exhibited the most severe IRI at 24 hrs after ROSC.[17,26] In our present work, NS group underwent CA/CPR without treatment of EGCG, and their brain tissue presents significantly decreased NDS, depressed ATPase activity and reduced ATP compared with the Sham group. And the remarkable increased openness of mPTP and obviously upregulated expression of cleaved-caspase 3 are also observed. These data indicate severe cerebral IRI and mitochondrial dysfunction.

EGCG is a kind of natural polyphenols which is isolated from green tea and it is able to accumulate in mitochondria to exert its biological effect.[13] EGCG (5–50 μm) dose-dependently inhibited ROS production and cytochrome c (cyto c) release and downregulated apoptosis-related protein expression in human dental pulp cells.[27] Similarly, a study on neurons showed that EGCG (5–20 μm) exhibits protective activity against apoptosis induced by mitochondrial oxidative stress.[13] By contrast, the opposing results of EGCG on mitochondrial function have been also reported. In Jurkat cells, EGCG (12.5–50 μm) promoted ROS generation and enhanced caspase-3 activity.[28] In addition, osteoclastic cell death was induced by ROS produced by EGCG (12.5–100 μm).[29] It had also been demonstrated that EGCG (0.5 mM) increased ROS generation, the mPTP opening as well as apoptosis level in HepG2 cells.[30] We hold the opinion that the various and opposing effects of EGCG may depend on the different dosage, cellular condition and cell types. Therefore, it is necessary to determine the effect of EGCG at certain dosage in each specific pathology conditions for precision medicine. By now, there are few studies demonstrating how EGCG affects the cerebral IRI post-CA/CPR. Our model simulates the clinical condition of CA/CPR, which composes of two phases, ischemia and reperfusion (IR). The cerebral injury caused by IR is rapidly progressive because there is significant cerebral injury following CA/CPR within a few minutes. EGCG (3 and 9 mg/kg) dose-dependently improves mitochondria dysfunction, as indicated by relieved oxidative stress, reduced mPTP opening degrees and downregulated apoptosis. However, it is not clear whether higher dosage of EGCG might aggravate cerebral IRI post-CA/CPR. Therefore, it still needs further investigation to evaluate the pharmacological action of EGCG in a CA/CPR model.

ERK signal pathway takes part in the modulation of cellular apoptosis and survival. Excessive p-ERK companied with IRI was observed in the CA/CPR model of rats. PD98059, a specific inhibitor of ERK, can effectively downregulate p-ERK level, reduce apoptosis, improve mitochondrial function and restore neural function, which marked the association between ERK upregulation and IRI after CA/CPR.[17,18] Another brain damage model established by MCAO exhibits focal brain damage. Several studies linked the focal cerebral IRI to the depressed p-ERK expression in a MCAO model. Experimental treatment which promoted the elevation of p-ERK could help neural function recovery and contributed to alleviation of IRI.[19–21] The underlying mechanism of cerebral injury may be different between the two models due to their inducement, pathophysiological reaction and the evaluation time point. On the other hand, it has been reported that ERK signal pathway can be regulated by EGCG.[31,32] To verify whether ERK pathway was involved in the mechanism by which EGCG alleviated cerebral IRI after CA/CPR, we extended our study to detect the ERK expression. The present results showed that EGCG treatment exhibits similar effect of PD98059, as indicated by decreasing the p-ERK expression, restoring mitochondrial function and improving the animals' neural function. These findings suggest the downregulation of ERK by EGCG is involved in the cerebral protective mechanism.

Recently, increasing reports about the clinical usage of EGCG have been published. Polyphenon E, primarily consisting of EGCG, is on the stage of clinical trial to test the effect on patients prior to bladder cancer surgery.[33] EGCG could potentially be used as a supplement of traditional rt-PA treatment among stroke patients to extend the narrow therapeutic window and improve the outcome in late stroke treatment.[34] The synergistic effect of EGCG and nifedipine is proved to be both safe and effective against pregnancy-induced severe pre-eclampsia.[35] In the present study, we hope our finding might provide the evidence which can support EGCG as a potential agent for treatment against cerebral IRI after CA/CPR in the future.

Conclusion

EGCG alleviated global cerebral ischemia/reperfusion injury by restoring mitochondrial dysfunction and ERK modulation

in a rat CA/CPR model, which might make it a potential candidate agent against IRI after CA/CPR in the future. Further study is needed to determine whether higher dosage of EGCG might aggravate cerebral IRI post-CA/CPR.

Disclosure

The authors report no conflicts of interest in this work.

References

1. Aronowski J, Strong R, Grotta JC. Reperfusion injury: demonstration of brain damage produced by reperfusion after transient focal ischemia in rats. *J Cereb Blood Flow Metab*. 1997;17(10):1048–1056. doi:10.1097/00004647-199710000-00006
2. Schaller B, Graf R. Cerebral ischemia and reperfusion: the pathophysiologic concept as a basis for clinical therapy. *J Cereb Blood Flow Metab*. 2004;24(4):351–371. doi:10.1097/00004647-200404000-00001
3. Del Castillo J, Lopez-Herce J, Canadas S, et al. Cardiac arrest and resuscitation in the pediatric intensive care unit: a prospective multicenter multinational study. *Resuscitation*. 2014;85(10):1380–1386. doi:10.1016/j.resuscitation.2014.06.024
4. Bosson N, Kaji AH, Koenig W, et al. Re-examining outcomes after unsuccessful out-of-hospital resuscitation in the era of field termination of resuscitation guidelines and regionalized post-resuscitation care. *Resuscitation*. 2014;85(7):915–919. doi:10.1016/j.resuscitation.2014.04.001
5. Kuschner CE, Becker LB. Recent advances in personalizing cardiac arrest resuscitation. *F1000Research*. 2019;8. doi:10.12688/f1000research.17554.1
6. Merchant RM, Yang L, Becker LB, et al. Incidence of treated cardiac arrest in hospitalized patients in the United States. *Crit Care Med*. 2011;39(11):2401–2406. doi:10.1097/CCM.0b013e3182257459
7. Chen K, Schenone AL, Gheyath B, et al. Impact of hypothermia on cardiac performance during targeted temperature management after cardiac arrest. *Resuscitation*. 2019. doi:10.1016/j.resuscitation.2019.06.276
8. Zhang JC, Lu W, Xie XM, Pan H, Wu ZQ, Yang GT. Mild hypothermia attenuates post-resuscitation brain injury through a V-ATPase mechanism in a rat model of cardiac arrest. *Genet Mol Res*. 2016;15(2). doi:10.4238/gmr.15027729.
9. Feldenberg LR, Thevananther S, Del Rio M, de Leon M, Devarajan P. Partial ATP depletion induces Fas- and caspase-mediated apoptosis in MDCK cells. *Am J Physiol*. 1999;276(6):F837–F846.
10. Adikesavan G, Vinayagam MM, Abdulrahman LA, Chinnasamy T. (-)-Epigallocatechin-gallate (EGCG) stabilize the mitochondrial enzymes and inhibits the apoptosis in cigarette smoke-induced myocardial dysfunction in rats. *Mol Biol Rep*. 2013;40(12):6533–6545. doi:10.1007/s11033-013-2673-5
11. Belobrov S, Seers C, Reynolds E, Cirillo N, McCullough M. Functional and molecular effects of a green tea constituent on oral cancer cells. *J Oral Pathol Med*. 2019. doi:10.1111/jop.12914
12. Huang SM, Chang YH, Chao YC, et al. EGCG-rich green tea extract stimulates sRAGE secretion to inhibit S100A12-RAGE axis through ADAM10-mediated ectodomain shedding of extracellular RAGE in type 2 diabetes. *Mol Nutr Food Res*. 2013;57(12):2264–2268. doi:10.1002/mnfr.201300275
13. Schroeder EK, Kelsey NA, Doyle J, et al. Green tea epigallocatechin 3-gallate accumulates in mitochondria and displays a selective antiapoptotic effect against inducers of mitochondrial oxidative stress in neurons. *Antioxid Redox Signal*. 2009;11(3):469–480. doi:10.1089/ars.2008.2215
14. Zheng J, Ramirez VD. Inhibition of mitochondrial proton F0F1-ATPase/ATP synthase by polyphenolic phytochemicals. *Br J Pharmacol*. 2000;130(5):1115–1123. doi:10.1038/sj.bjp.0703397
15. Dragicevic N, Smith A, Lin X, et al. Green tea epigallocatechin-3-gallate (EGCG) and other flavonoids reduce Alzheimer's amyloid-induced mitochondrial dysfunction. *J Alzheimer's Dis*. 2011;26(3):507–521. doi:10.3233/JAD-2011-101629
16. Krishnan TR, Velusamy P, Mangaiah S, et al. Epigallocatechin-3-gallate restores the Bcl-2 expression in liver of young rats challenged with hypercholesterolemia but not in aged rats: an insight into its disparity of efficacy on advancing age. *Food Funct*. 2014;5(5):916–926. doi:10.1039/c3fo60345h
17. Nguyen Thi PA, Chen MH, Li N, Zhuo XJ, Xie L. PD98059 protects brain against cells death resulting from ROS/ERK activation in a cardiac arrest rat model. *Oxid Med Cell Longev*. 2016;2016:3723762. doi:10.1155/2016/3723762
18. Zheng JH, Xie L, Li N, et al. PD98059 protects the brain against mitochondrial-mediated apoptosis and autophagy in a cardiac arrest rat model. *Life Sci*. 2019;116618. doi:10.1016/j.lfs.2019.116618
19. Zhu YM, Wang CC, Chen L, et al. Both PI3K/Akt and ERK1/2 pathways participate in the protection by dexmedetomidine against transient focal cerebral ischemia/reperfusion injury in rats. *Brain Res*. 2013;1494:1–8. doi:10.1016/j.brainres.2012.11.047
20. Wang PR, Wang JS, Zhang C, Song XF, Tian N, Kong LY. Huang-Lian-Jie-Du-Decotion induced protective autophagy against the injury of cerebral ischemia/reperfusion via MAPK-mTOR signaling pathway. *J Ethnopharmacol*. 2013;149(1):270–280. doi:10.1016/j.jep.2013.06.035
21. Yang SI, Yuan Y, Jiao S, Luo QI, Yu J. Calcitonin gene-related peptide protects rats from cerebral ischemia/reperfusion injury via a mechanism of action in the MAPK pathway. *Biomed Reports*. 2016;4(6):699–703. doi:10.3892/br.2016.658
22. Chen MH, Liu TW, Xie L, et al. A simpler cardiac arrest model in rats. *Am J Emerg Med*. 2007;25(6):623–630. doi:10.1016/j.ajem.2006.11.033
23. Jia X, Koenig MA, Shin HC, et al. Improving neurological outcomes post-cardiac arrest in a rat model: immediate hypothermia and quantitative EEG monitoring. *Resuscitation*. 2008;76(3):431–442. doi:10.1016/j.resuscitation.2007.08.014
24. Lobo-Jarne T, Ugalde C. Respiratory chain supercomplexes: structures, function and biogenesis. *Semin Cell Dev Biol*. 2018;76:179–190. doi:10.1016/j.semcdb.2017.07.021
25. Circu ML, Aw TY. Reactive oxygen species, cellular redox systems, and apoptosis. *Free Radic Biol Med*. 2010;48(6):749–762. doi:10.1016/j.freeradbiomed.2009.12.022
26. Zhuo X, Xie L, Shi FR, Li N, Chen X, Chen M. The benefits of respective and combined use of green tea polyphenols and ERK inhibitor on the survival and neurologic outcomes in cardiac arrest rats induced by ventricular fibrillation. *Am J Emerg Med*. 2016;34(3):570–575. doi:10.1016/j.ajem.2015.12.011
27. Park SY, Jeong YJ, Kim SH, Jung JY, Kim WJ. Epigallocatechin gallate protects against nitric oxide-induced apoptosis via scavenging ROS and modulating the Bcl-2 family in human dental pulp cells. *J Toxicol Sci*. 2013;38(3):371–378.
28. Nakagawa H, Hasumi K, Woo JT, Nagai K, Wachi M. Generation of hydrogen peroxide primarily contributes to the induction of Fe(II)-dependent apoptosis in Jurkat cells by (-)-epigallocatechin gallate. *Carcinogenesis*. 2004;25(9):1567–1574. doi:10.1093/carcin/bgh168
29. Nakagawa H, Wachi M, Woo JT, et al. Fenton reaction is primarily involved in a mechanism of (-)-epigallocatechin-3-gallate to induce osteoclastic cell death. *Biochem Biophys Res Commun*. 2002;292(1):94–101. doi:10.1006/bbrc.2002.6622
30. Khiewkamrop P, Phunsomboon P, Richert L, Pekthong D, Srisawang P. Epistructured catechins, EGCG and EC facilitate apoptosis induction through targeting de novo lipogenesis pathway in HepG2 cells. *Cancer Cell Int*. 2018;18:46. doi:10.1186/s12935-018-0539-6
31. Wu DD, Liu ZG, Li JM, et al. Epigallocatechin-3-gallate inhibits the growth and increases the apoptosis of human thyroid carcinoma cells through suppression of EGFR/RAS/RAF/MEK/ERK signaling pathway. *Cancer Cell Int*. 2019;19. doi:10.1186/s12935-019-0762-9

32. Yamamoto N, Shibata M, Ishikuro R, et al. Epigallocatechin gallate induces extracellular degradation of amyloid beta-protein by increasing neprilysin secretion from astrocytes through activation of ERK and PI3K pathways. *Neuroscience*. 2017;362:70–78. doi:10.1016/j.neuroscience.2017.08.030
33. Gee JR, Saltzstein DR, Kim K, et al. A Phase II randomized, double-blind, presurgical trial of polyphenon E in bladder cancer patients to evaluate pharmacodynamics and bladder tissue biomarkers. *Cancer Prev Res*. 2017;10(5):298–307. doi:10.1158/1940-6207.CAPR-16-0167
34. Wang XH, You YP. Epigallocatechin gallate extends therapeutic window of recombinant tissue plasminogen activator treatment for brain ischemic stroke: a randomized double-blind and placebo-controlled trial. *Clin Neuropharmacol*. 2017;40(1):24–28. doi:10.1097/WNF.0000000000000197
35. Shi DD, Guo JJ, Zhou L, Wang N. Epigallocatechin gallate enhances treatment efficacy of oral nifedipine against pregnancy-induced severe pre-eclampsia: a double-blind, randomized and placebo-controlled clinical study. *J Clin Pharm Ther*. 2018;43(1):21–25. doi:10.1111/jcpt.12597